Eur Radiol (2003) 13:1538–1548
DOI 10.1007/s00330-002-1811-6

PEDIATRIC

The value of fast MR imaging as an adjunct to ultrasound in prenatal diagnosis

L. Breysem
H. Bosmans
S. Dymarkowski
D. Van Schoubroeck
I. Witters
J. Deprest
P. Demaerel
D. Vanbeckevoort
C. Vanhole
P. Casaer
M. Smet

Received: 4 June 2002
Revised: 14 October 2002
Accepted: 6 December 2002
Published online: 15 April 2003

L. Breysem (✉) · H. Bosmans
S. Dymarkowski · P. Demaerel
D. Vanbeckevoort · M. Smet
Department of Radiology,
University Hospitals,
Herestraat 49, 3000 Leuven, Belgium
e-mail: luc.breysem@uz.kuleuven.ac.be
Tel.: +32-16-343765
Fax: +32-16-343782

D. V. Schoubroeck · I. Witters · J. Deprest
Department of Obstetrics and Gynecology,
University Hospitals,
Herestraat 49, 3000 Leuven,
Belgium

C. Vanhole · P. Casaer
Department of Pediatrics,
University Hospitals,
Herestraat 49, 3000 Leuven,
Belgium

Abstract The aim of this study was to evaluate the role of MR imaging of the fetus to improve sonographic prenatal diagnosis of congenital anomalies. In 40 fetuses (not consecutive cases) with an abnormality diagnosed with ultrasound, additional MR imaging was performed. The basic sequence was a T2-weighted single-shot half Fourier (HASTE) technique. Head, neck, spinal, thoracic, urogenital, and abdominal fetal pathologies were found. This retrospective, observational study compared MR imaging findings with ultrasonographic findings regarding detection, topography, and etiology of the pathology. The MR findings were evaluated as superior, equal to, or inferior compared with US, in consent with the referring gynecologists. The role of these findings in relation to pregnancy management was studied and compared with postnatal follow-up in 30 of 40 babies. Fetal MRI technique was successful in 36 of 39 examinations and provided additional information in 21 of 40 fetuses (one twin pregnancy with two members to evaluate). More precise anatomy and location of fetal pathology (20 of 40 cases) and additional etiologic information (8 of 40 cases) were substantial advantages in cerebrospinal abnormalities [ventriculomegaly, encephalocele, vein of Galen malformation, callosal malformations, meningo(myelo)-cele], in retroperitoneal abnormalities (lymphangioma, renal agenesis, multicystic renal dysplasia), and in neck/thoracic pathology [cervical cystic teratoma, congenital hernia diaphragmatica, congenital cystic adenomatoid lung malformation (CCAM)]. This improved parental counseling and pregnancy management in 15 pregnancies. In 3 cases, prenatal MRI findings did not correlate with prenatal ultrasonographic findings or neonatal diagnosis. The MRI provided a more detailed description and insight into fetal anatomy, pathology, and etiology in the vast majority of these selected cases. This improved prenatal parental counseling and postnatal therapeutic planning.

Keywords MR imaging · Fetal brain · Fetal neck · Fetal chest · Fetal abdomen · Fetal urinary tract

Introduction

Magnetic resonance imaging is a superior imaging modality for many diagnostic problems. Images can be obtained in any orientation and the soft tissue contrast is excellent. Continuous technical improvements have led to subsecond acquisition schemes that provide T1- and T2-weighted images with a relatively high in-plane resolution. In the frame of fetal imaging, the lack of ionizing radiation is an additional advantage. No adverse magnetic effects on fetal growth or development are reported in the literature [1, 2, 3, 4]. These factors make MRI a

promising and already accepted modality to image the fetus and fetal pathology of the different organ systems [5, 6, 7, 8, 9].

Currently, two main tasks have to be addressed. The image quality has to be studied for the specific applications in fetal MRI and good indications have to be formulated. Many authors report their experience on the subject and each article has contributed to further specification of the indications for MR imaging of the fetus [5, 6, 7, 8, 9].

In our department, an MRI of the fetus is performed when a sonographic abnormality is detected and further diagnostic information is considered useful in pregnancy management. We reviewed retrospectively our cases of the past 5 years and evaluated the value of MRI with regard to diagnostic information and its influence in further decision making as well as parental counseling. Since the pathology is diverse and the number of patients of each pathology is limited, statistical analysis of our observations could not be performed.

The purpose of this article is a retrospective, observational analysis of US and MRI abnormalities in selected prenatal pathology.

Materials and methods

From 1996 to 2001, fetal abnormalities detected on US were further investigated with MRI in 38 pregnant women (mean age 28 years, age range 18–41 years): 5 twin pregnancies and 33 singletons. Only in one twin pregnancy did the two members have to be investigated. In the other four twin pregnancies, we examined thoroughly only the indicated member in order to limit the examination time. One patient with fetofetal transfusion syndrome was investigated before and after treatment of the transfusion syndrome. Finally, 40 fetuses were investigated with US and MRI. Mean gestational age (GA) was 28.3 weeks (range 19–39 weeks).

The cases were selected with prenatal ultrasound. The main objective of the additional MR imaging was to complete or to further specify ultrasonographic abnormalities. The diagnostic problem was discussed in advance by a multidisciplinary board of radiologists, gynecologists with experience in ultrasonography, and neonatologists.

Before the examination, all patients were orally informed about the procedure and the safety of the technique as reported thus far in the literature and all provided their informed consent.

Abnormal prenatal US findings selected for additional MRI concerned different anatomical regions of the fetus such as central nervous system pathology, neck pathology, as well as thoracic and abdominal or retroperitoneal abnormalities. In 1 patient there was associated maternal and fetal abnormality (Table 1).

All magnetic resonance examinations were performed on 1.5-T MR systems, either a 1.5-T Siemens Vision system (14 cases; Siemens, Erlangen, Germany) or a 1.5-T Philips Gyroscan system (25 cases; Philips, Best, The Netherlands). The body phased-array coil was used in all cases.

The women were positioned in decubitus dorsalis or on the left side to improve their comfort during the examination. Ultrafast imaging techniques were used in all patients. The basic sequence for the studies on the 1.5-T Siemens Vision system was a T2-weighted half-Fourier single-shot turbo spin-echo (HASTE) acquisition that acquires two consecutive images after a single radiofrequency excitation pulse [10]. The first image had an echo time of 60 ms, and the second image had an echo time of 400 ms. This particular sequence was not available on the 1.5-T Philips Gyroscan system; instead, we used a single-shot HASTE acquisition with effective echo time of 60 ms and a single-shot rapid acquisition with relaxation enhancement (RARE) acquisition of the same location using an echo time of 1 s. Other parameters for all HASTE acquisitions were identical for both the Siemens and the Philips systems: matrix 160×256, echo spacing 4.2 ms, bandwidth 650 Hz/pixel, slice thickness 27 mm and refocusing pulse 120–160°. The field of view was set at the minimal possible value and depended strongly on the chosen orientation. The RARE acquisition had a matrix of 256×256, slice thickness as in the HASTE acquisition, bandwidth 395 Hz/pixel and echo spacing of 7.8 ms. In addition to these sequences, other techniques were explored to increase image resolution, to improve image contrast, or to obtain T1-weighted images. Other T2-weighted acquisitions included multishot turbo-spin-echo techniques (echo train length of 65 echoes, image matrix 256×512, TE 120 ms, bandwidth 580 Hz/pixel), and true fast imaging with steady precession (FISP) measurements (TR 6.3 ms, TE 3.0 ms, flip angle 70°). In 1 patient a single-shot myelography acquisition was performed (TE 1 s,

Table 1 Ultrasound indications for additional fetal MRI. *CNS* central nervous system; *CMV* cytomegalovirus

CNS abnormalities	Twin-to-twin transfusion syndrome before (*n*=1) and after laser coagulation (*n*=1) Unilateral ventriculomegaly (*n*=3) Bilateral ventriculomegaly (including colpocephaly and/or suspicion of fossa posterior anomaly; *n*=8) Vein of Galen malformation (*n*=1) CMV reactivation (*n*=2) Encephalocele (*n*=1) Facial dysmorphy with cleft lip (*n*=1) Lumbosacral cyst (*n*=3)
Neck pathology	Large cystic mass in the neck (*n*=2)
Thoracic pathology	Congenital hernia diaphragmatica (*n*=3) Unilateral hyperechoic lung (*n*=1) Lung cyst (*n*=1)
Abdominal or retroperitoneal pathology	Intraabdominal cystic mass (*n*=5) Evaluation of the kidneys in assessment of renal agenesis (*n*=4) Urethral valves with vesicoamniotic shunt (*n*=1)
Placental and fetal pathology	Placental chorangiomas and enlarged fetal organs (*n*=1)

slice thickness 10 mm, matrix 256×256). T1-weighted images were obtained with turbo fast low-angle shot (FLASH) measurement (TR 7 ms, TE 4 ms, inversion recovery time 300 ms) and 2D FLASH acquisitions using fat suppression (TE 5 ms, TR 230 ms). These additional measurements were performed in 2 patients each.

The HASTE acquisitions were performed in the fetal axial, sagittal, and coronal acquisition planes. Imaging time of the examination varied between 30 and 45 min.

Oral sedation (flunitrazepam 1 mg) was used in 4 cases, in consent with the gynecologist. Indications were a very mobile fetus in early pregnancy (second trimester) on ultrasound or when the mother was very anxious. In 30 of 40 babies, follow-up is available.

Results

Image quality

The examination had to be aborted in 1 case because of claustrophobia. Images were inconclusive in 1 obese woman probably because the body phased-array coil could not be used. The fetus had a large cystic mass in the oropharynx or neck region on US, which unfortunately could not be clarified with MRI (Fig. 1). After birth, an immature cystic grade-II teratoma, originating from the palate, was diagnosed at surgery and histology.

Movement of the fetus was present in 5 cases, but in only 1 was diagnostic imaging not possible because of motion artifacts. In one fetus with a ventrally lying head, it was impossible to overcome image artifacts and images were partially inconclusive.

Fig. 1 Sagittal T2-weighted single-shot half-Fourier (HASTE; TE 60 ms) image of an obese woman: insufficient diagnostic quality in this fetus (GA 28 weeks) to evaluate a large cystic mass centered at the mouth

Imaging technique

True axial, sagittal, and coronal planes were obtained in all other fetuses except in 4, owing to the difficult fetal position. The suboptimal examinations still provided images with an acceptable image quality.

Regarding the imaging technique, the HASTE acquisition that provides both a short and a long TE image gave the best result. In the additional true-FISP (3 cases) and multishot turbo-spin-echo images (1 case), we observed more noise. Although the image matrix was higher than in the HASTE acquisition, there was no benefit on the apparent image resolution. These extra sequences were complementary to the HASTE acquisition and no fetus had to be excluded from the evaluation.

The image with long TE shows tissues with long T2 with hyperintense signal intensities. The advantage in fetal imaging consists of the enhancement of fluid-filled structures. These anatomical structures can be clearly delineated and can thus be used as landmarks. In fetal pathology, this technique was best appreciated for evaluation of the cerebrum to evaluate the ventricles and the subarachnoidal space at the convexity of the brain or in the fossa posterior. Fluid-filled structures in the lungs, e.g., visualization of CCAM (Fig. 2) and in the spinal canal, were other anatomical structures which benefit from images with long T2. In 1 patient images of the spinal canal were completed with a single-shot myelography acquisition and demonstrated very clearly the connection between a lumbar cyst and the spinal canal (Fig. 3; Table 2).

In our study group, pathology of the cerebrum (n=19) and spinal canal (n=3) was most frequent. Owing to the MRI characteristics as mentioned above, evaluation of the sulci-gyri and fossa posterior was superior with MRI compared with US in all cases. The US evaluation of the fossa posterior can be difficult (osseous superposition, suboptimal fetal position). With MRI, cerebellar hemispheres, vermis, subarachnoidal space, and fourth ventricle are visible. In most fetuses with ventriculomegaly, there were neither associated anomalies found in the parenchyma nor in the fossa posterior. In 1 patient with bilateral ventriculomegaly, there was a very small clot visible in the lateral ventricle as a hypointense spot on T2 sequence, suggesting post-hemorrhagic hydrocephalus, confirmed with postnatal ultrasound. Fetal MRI at 34 weeks GA was able to detect a parenchymal defect in a fetus with cytomegalovirus (CMV) reactivation and ventriculomegaly, postnatally confirmed with neonatal CT and MRI of the brain at the age of 3 months. The MRI at 3 months of age showed periventricular white matter lesions, probably as a result of CMV infection (Fig. 4).

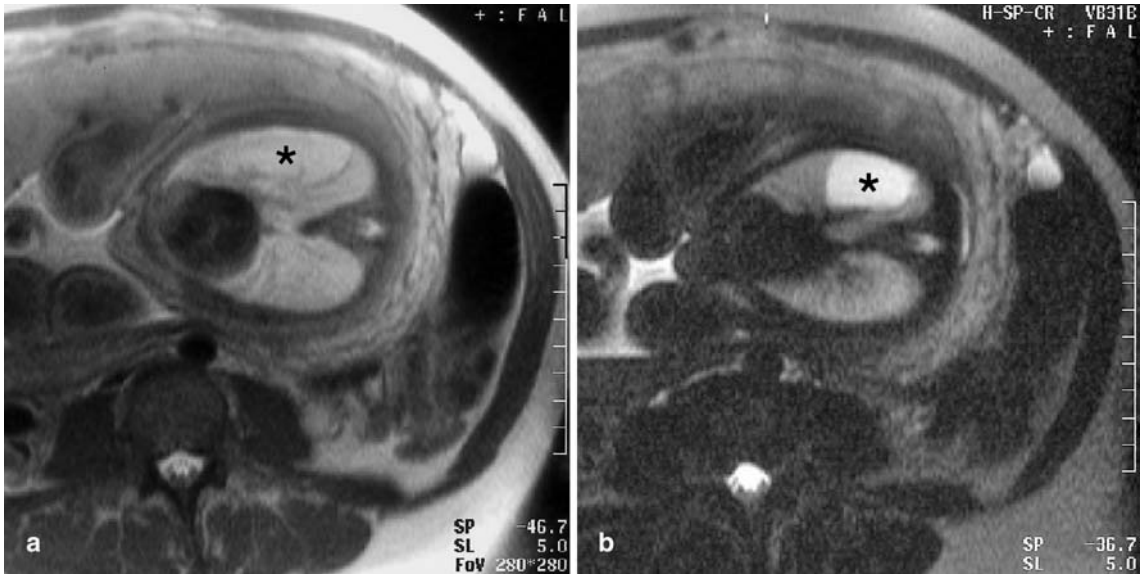

Fig. 2a, b Axial T2-weighted HASTE (**a** TE 60 ms, **b** TE 400 ms), 5-mm slice thickness: visualization and delineation between normal lung tissue and a cystic lesion (*asterisks*) is better seen on the image with late TE in this fetus (GA 36 weeks) with confirmed congenital cystic adenomatoid lung malformation

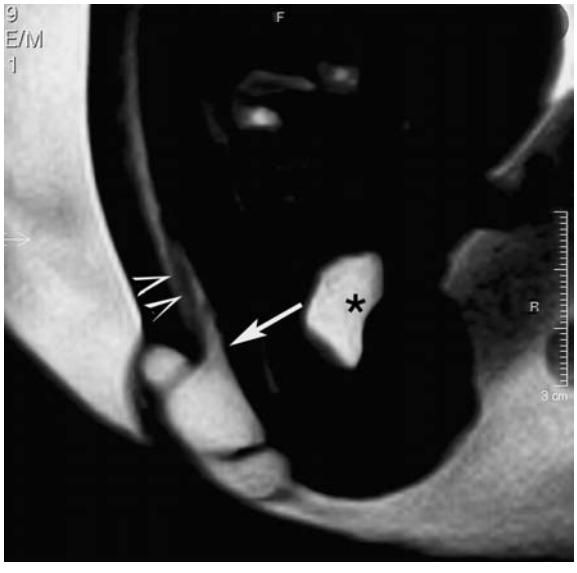

Fig. 3 Sagittal, heavily T2-weighted single-shot myelography acquisition: the connection (*arrow*) between the sacral cyst and the subarachnoidal space in the spinal canal is clearly seen in this fetus (GA 22 weeks). The bladder can serve as landmark (*asterisk*). The hypointense linear structure seen in the sacral spinal canal is the tethered cord, confirmed surgically

In 1 case with an enlarged fossa posterior and moderate dilatation of the ventricles on US, there was striking cerebellar hypoplasia and inappropriate cortical gyration for fetal age (33 weeks). A few days later, bilateral parenchymal hyperreflections could be demonstrated on US as a result of severe CMV infection (Fig. 5). These findings were not appreciated on MRI. No autopsy was performed.

Callosal agenesis was demonstrated in 1 patient with colpocephaly, basically on the secondary signs of abnormal ventricular morphology.

Useful additional information was provided with MRI in other congenital brain malformations such as a large encephalocele (*n*=1; Fig. 6): a global overview of the malformation, visualization of the internal structure of the cele and a Chiari malformation, and suspicion of midline malformation were additional findings on MRI. Small choroidal and perforant veins were demonstrated in 1 case with an aneurysm on the vein of Galen.

The connection with the lumbar spine was demonstrated in 2 of 3 patients with a suspicion of meningomyelocele on US and diagnosis could be confirmed postnatally (Table 3).

The anatomical position of intraabdominal cystic masses (*n*=5) was better evaluated in 2 cases, compared with the US findings. A septated cyst, on prenatal US possibly related to the kidneys, could be diagnosed with MRI as a retroperitoneal lymphangioma just beneath the right kidney (Fig. 7). In the other case, US was suggestive for multicystic renal dysplasia but could be confirmed with great certainty with the additional MRI images.

Exploration of the renal area in cases of suspected renal agenesis (*n*=4) was possible. Important conclusions, such as renal agenesis or renal presence, could be confirmed with MRI.

In the case with megacystis, bilateral hydronephrosis, and diagnosis of urethral valves, the valves could not be demonstrated but, equal to US, hydronephrosis was visible. In addition, the differentiation between adrenal hemorrhage and a cystic lesion in the kidney upper pole, as suspected on US, could be made with MRI (Table 4).

Table 2 Central nervous system pathology. *MMC* meningomyelocele

Gestational age (weeks)	US indication	MRI findings	Outcome/follow-up
25	Twin-to-twin transfusion Acardiacus Before laser therapy	Normal	
27	After laser therapy	Normal	No follow-up
19	Twin-to-twin transfusion After laser therapy Cystic leukomalacia on donor: mors in utero Recipient: Bilateral ventriculomegaly Hemorrhage? White matter?	No additional findings No associated anomalies	4 days after MRI Prenatal US
18	Twin-to-twin transfusion Stuck twin Both members: borderline Bilateral ventriculomegaly	Mild ventriculomegaly in both members No associated anomalies	Normal twins
38	Twin One member: moderate hydrocephaly, no septum pellucidum visible: Holoprosencephaly? Corpus callosum? Other?	Corpus callosum present Thin septum pellucidum: Long-existing hydrocephaly?	Postnatal US, MRI, CT: aqueductal stenosis
30	Unilateral ventriculomegaly	No associated anomalies	No follow-up
33	Unilateral ventriculomegaly	No associated anomalies	Normal; no further imaging available
34	Bilateral ventriculomegaly	Small unilateral intraventricular cloth	Post-hemorrhagic hydrocephaly on postnatal US and CT Conservative treatment
28	Bilateral ventriculomegaly	No associated anomalies	Postnatal US and CT: lateral hydrocephaly Ventricular peritoneal drain Minor cerebral palsy and axial hypotonia
33	Enlarged fossa posterior Mild hydrocephaly Irregular ventricle wall	Colpocephaly Cortical migration anomaly Dandy-Walker variant?	Deceased No autopsy results CMV infection
34	Unilateral ventriculomegaly CMV reactivation	Unilateral ventriculomegaly Ipsilateral white matter lesion	Postnatal CT and MRI at 3 months of age: confirmation of white matter lesion, small intraventricular hemorrhage and hydrocephaly
27	CMV reactivation	No associated or additional findings	No follow-up
33	Colpocephaly	Partial or complete callosal agenesis	Postnatal US and MRI: callosal agenesis
35	Cleft lip Facial dysmorphy Cerebral cleft?	No associated anomalies	No follow-up
30	Encephalocele fossa posterior?	Occipital encephalocele Arnold-Chiari type II Cortical development anomaly	Deceased Autopsy: encephalocele, Arnold-Chiari type II No microscopy available
33	Vein of Galen malformation Small veins? Type?	Vein of Galen malformation of the choroidal type	Deceased No autopsy results
36	At lumbar level: cystic lesion No spinal communication Cystic teratoma? Meningocele?	No additional findings	MMC
39	MMC? No visible spinal communication	Spinal communication is visible: MMC with tethering	MMC with tethering at surgery
26	Sacral cyst MMC?	Spinal communication is visible: MMC?	MMC

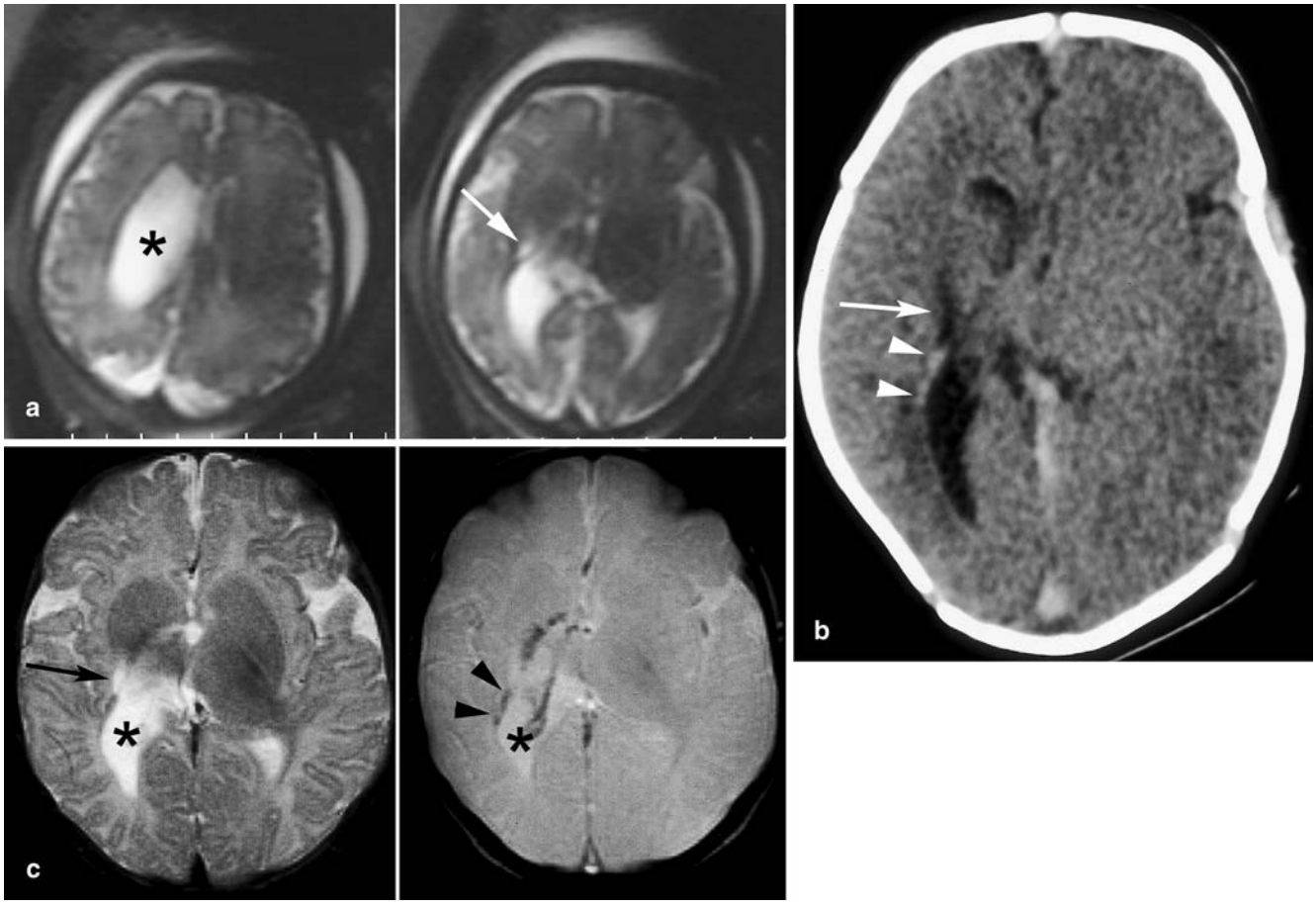

Fig. 4a–c Ventriculomegaly and cytomegalovirus (CMV) reactivation, at 34 weeks. **a** Axial T2-weighted HASTE (TE 378 ms): right-sided unilateral ventriculomegaly (*asterisk*); ipsilateral periventricular small hyperintense lesion (*arrow*) compatible with small infarct/gliosis. **b** Postnatal CT on day 6: right-sided unilateral ventriculomegaly with intraventricular hyperintense material compatible with hemorrhage (*arrowheads*) and a periventricular hypodense lesion (*arrow*) compatible with small infarct and comparable with the lesion seen on prenatal MRI. **c** Axial T2-weighted and T2* gradient-echo MRI at 3 months of age: sequelae of the same right sided periventricular small infarct (*arrow*) and hemorrhage (*arrowhead*; gradient echo) with unilateral ventriculomegaly (*asterisk*)

Magnetic resonance imaging demonstrated the extent and content of diaphragmatic herniation (n=3) and, in addition, position of the liver and volume of the ipsi- and contralateral lung.

The relation of the upper airways to giant neck mass (n=1; Fig. 8) and evaluation of bronchial atresia in a fetus with a unilateral hyperechoic lung (n=1) was superior with MRI compared with US. This resulted in optimal prenatal and postnatal therapeutic management. The final diagnosis was respectively a mature cystic teratoma in the neck and a CCAM, which regressed spontaneously. One case with a cystic lung malformation on US was visible in more detail on the heavily T2-weighted images: septations and small surrounding cysts were visible and was very suggestive of a cystic adenomatoid lung malformation, type II, confirmed postnatally with CT and pathology.

Influence on management

Overall, when additional information was demonstrated or the sonographic findings could be confirmed with great certainty, parental counseling was more accurate. Magnetic resonance was an additional tool for the gynecologist in 5 cases when difficult therapeutic decisions about whether to offer termination of pregnancy (TOP; n=4) or, in a twin-to-twin transfusion syndrome, proceed with a planned laser coagulation, were the issue. In 1 case with a confirmed meningomyelocele (MMC) on MRI, multidisciplinary prenatal counseling was optimized towards the parents.

In 3 cases prenatal MRI findings did not correlate with prenatal or postnatal ultrasonographic abnormalities and/or neonatal diagnosis: one fetus with CMV infection had calcifications and thalamostriate vasculopathy on prenatal US, performed at the time of the MRI; a pregnancy

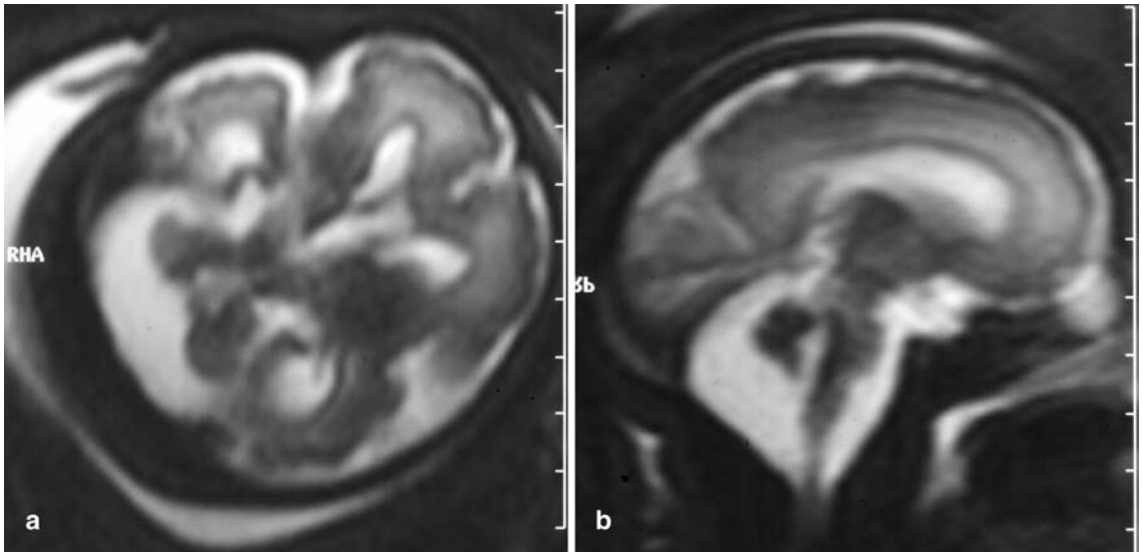

Fig. 5 **a** Sagittal and **b** axial T2-weighted HASTE (TE 60 ms): bilateral ventricular dilatation, irregular cortical ribbon. Gyration is not compatible with the GA; most striking is the cerebellar hypoplasia seen in this fetus with CMV (GA 33 weeks)

Table 3 Abdominal and urogenital pathology

Gestational age (weeks)	US indication	MRI findings	Outcome/follow-up
25	Placental chorangiomas, enlarged fetal organs: Tumor?	No tumoral lesion Enlarged fetal organs Placental hemangiomas	Deceased Pathology: Beckwith-Wiedeman syndrome
35	Cyst in right hemi-abdomen	No additional findings	No follow-up
39	Septated cystic lesion in right upper quadrant: Gastrointestinal? Renal?	Retroperitoneal septated cyst, extrarenal: compatible with lymphangioma	Conservative treatment
32	Subdiaphragmatic intraabdominal cyst, residual lesion after punction?	No cyst visible	No treatment No cyst on postnatal imaging
33	Large multicystic intraabdominal structure: Renal? Extrarenal?	Multicystic renal dysplasia on the left	Postnatal US: confirmation Conservative follow-up
22	Complex cystic malformation intraabdominal: Renal? Extrarenal?	Confirmation of the cystic mass, no additional diagnostic information	Deceased Pathology: Vater syndrome
34	IUGR Anamnion Kidney present?	Fetal kidneys present	Mors in utero (35 weeks) Pathology: vena subchorea thrombosis, aberrant insertion of the umbilical cord
22	Oligohydramnion kidneys? Familial history of Potter sequence	Fetal kidneys present	Normal follow-up
34	Renal agenesis	Confirmation No additional findings	Pathology: Potter sequence
29	Diaphragmatic hernia Kidneys present?	Kidneys absent	Pathology: kidneys absent
24	Megabladder	Confirmation of urogenital pathology	Urethral valves and obstructive uropathy on US, cystogram, and scintigraphy
	Bilateral hydronephrosis, urethral valves	Shunt not visible	Evolution: end stage
	Vesicoamniotic shunt Right renal cyst Placental hemorrhage	Adrenal hemorrhage, no renal cyst	Renal failure, right nephrectomy

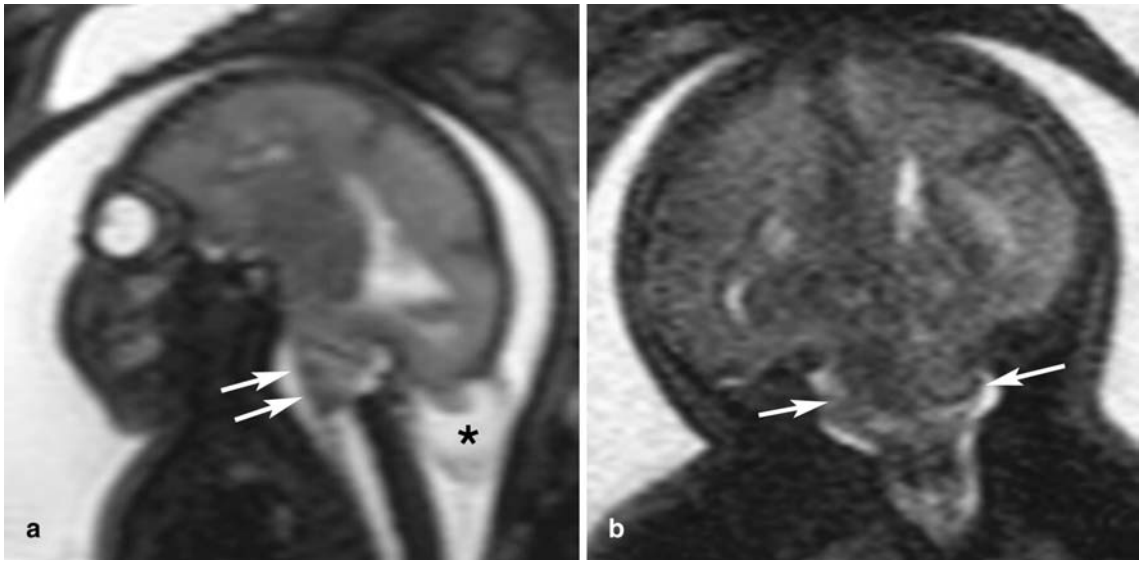

Fig. 6 **a** Sagittal and **b** coronal heavily T2-weighted HASTE (TE 400 ms): Chiari type-II malformation (*arrows*) is appreciated on the fetal MRI in this fetus (GA 30 weeks) with a large encephalocele (*asterisk*). Gyration is not compatible with fetal age: the cortex appears abnormally smooth and few sulci are visible, and the subarachnoidal space is not visible. No autopsy results were available

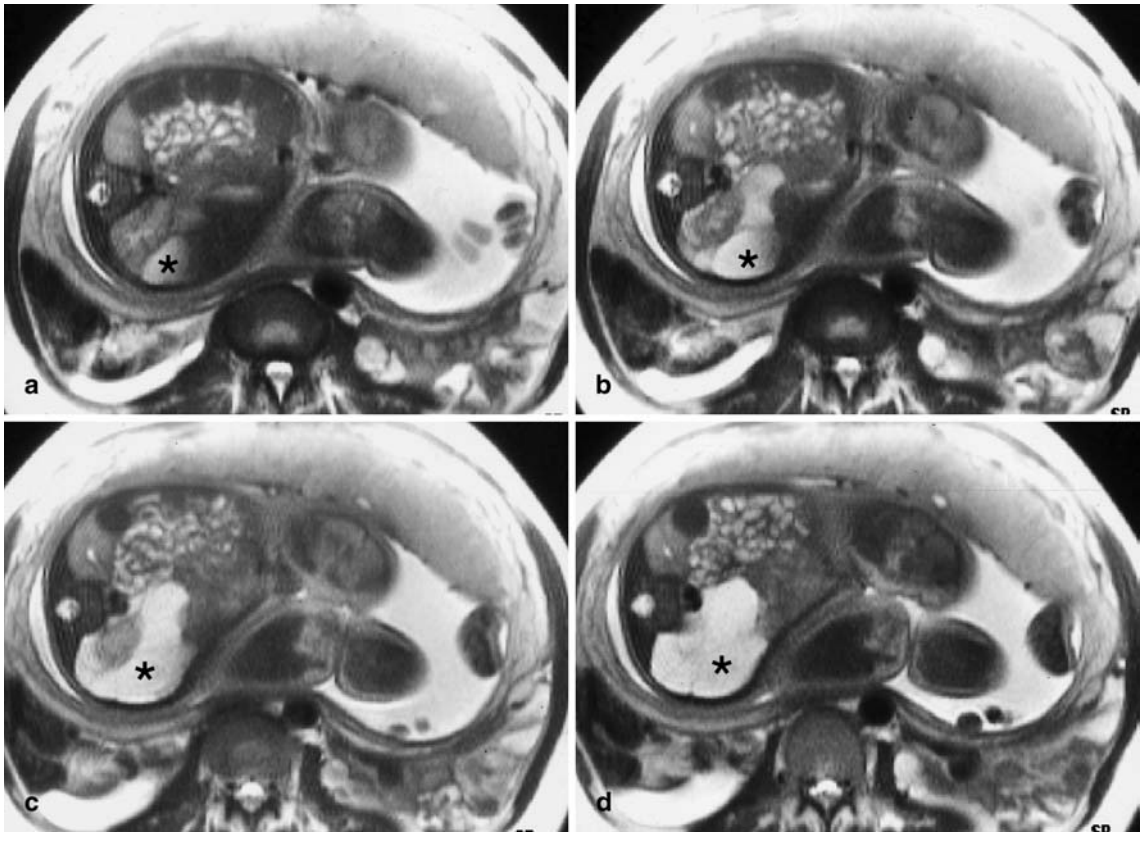

Fig. 7a–c Craniocaudal migration, axial T2-weighted images, slice thickness 6 mm: MRI demonstrates that the retroperitoneal septated cystic mass (*asterisk*) surrounds, but does not affect, the right kidney. Diagnosis: retroperitoneal lymphangioma

Fig. 8 Coronal T2-weighted HASTE (TE 60 ms): MRI clearly demonstrates the anatomical relationship between the pharynx (*arrow*) and the septated cystic mass on the right (*asterisk*): this optimized prenatal and postnatal approach (histology: mature cystic teratoma)

with fetofetal transfusion after laser coagulation developed cystic periventricular leukomalacia in one member, not visible on the MR images but seen on US 4 days after the fetal MRI. The TOP was carried out after US findings and no autopsy results were available. A third case with a posterior extracorporeal cyst at high lumbar level without demonstrable connection with the spinal canal on US or on MRI finally proved to be an MMC.

Discussion

Optimal diagnosis of prenatal abnormalities is necessary to assure an adequate prenatal and postnatal management and parental counseling. Ideally, diagnosis is made with a non-invasive imaging method.

Prenatal US remains the primary imaging method to explore the fetus because it is safe, easily accessible, and inexpensive. Notwithstanding the use of high-resolution US and very sensitive Doppler techniques, unsolvable questions remain [11]. In this group, MRI finds its indications, as this is also a safe and non-invasive modality.

Although no adverse effects have been reported in the literature up to now, most authors recommend limiting the examination time and not performing the examinations during the first trimester [1, 2, 4, 12, 13]. With respect to further pregnancy management, the second-trimester age group is of the utmost importance. At that GA, the fetus is small and relatively mobile and providing good-resolution images remains a challenge in MR imaging. Even in the third trimester, suboptimal resolution can influence diagnostic quality. In a 32-week-old fetus with congenital hernia diaphragmatica (CHD), we were unable to localize the position of the liver correctly

Table 4 Neck and chest pathology

Gestational age (weeks)	US indication	MRI findings	Outcome/follow-up
26	Enlarged echogenic left lung: Sequester? Bronchial atresia? Cyst?	Bronchial tree: normal	Congenital lung malformation: resolved spontaneously
	No “large” cyst	Unilateral large hyperintense lung	CT: no cysts
31	Lung cyst unilateral Further differentiation?	Lung cyst Small peripheral cysts: compatible with CCAM	Postnatal CT and surgery: CCAM
30	Large cervical septated cystic mass	Relation to the airways is seen clearly Lymphangioma?	Surgery Histology: mature cystic teratoma
22	CHD Liver? Lung volume?	CHD Liver “up”	No follow-up
32	CHD Liver? Lung volume?	CHD Liver “up”	No follow-up
32	CHD Liver? Lung volume?	CHD Liver “up”	Deceased Pathology: confirmation Liver partially intrathoracic

Fig. 9 Axial T2-weighted HASTE (TE 400 ms): the brain of an 18-week-old fetus, member of a monochorionic twin pregnancy with significant fetofetal transfusion (US diagnosis), before laser coagulation: the three normal anatomical layers (ependyma, white matter and cortex) of the fetal brain are clearly seen; the smooth cortical layer, as well as the prominent subarachnoidal space and lateral ventricles, are normal for gestational age

on the MR images due to suboptimal quality of the images in the area of interest.

In our department, MRI is considered when the US findings are equivocal or when the US images are difficult to interpret such as in late pregnancy or with an inaccessible fetal position. The medical diagnosis was discussed in advance on a multidisciplinary basis.

The latest ultra-fast imaging techniques were used throughout this study. They provided two major advantages: image acquisition time was short and motion of the fetus did not usually degrade image quality [10, 14].

In the initial phase of the study, we tried techniques other than HASTE. Because of the limited number of patients, the findings were only observational: none of the alternatives, including multi-shot turbo spin-echo, true FISP, T1-weighted turbo FLASH, and T1-weighted FLASH with fat suppression, seemed to be an improvement in our patients. Only in one article was true FISP preferred to evaluate fetal pathology [15]. On the other hand, high-quality images were delivered with HASTE acquisitions using a slice thickness of 2 mm. This was most obvious in the images of the brain in an 18-week-old fetus in a twin-to-twin transfusion syndrome (Fig. 9). This case demonstrates the normal anatomy of a fetal brain: the multilayered pattern; the smooth surface of the brain without sulci and gyri; prominent lateral ventricles; and subarachnoidal space [16, 17]. In the other cases, slice thickness varied between 4 and 7 mm.

A large field of view in MR imaging can offer a global overview of the fetal pathology or anatomy. In that respect some cases benefit from MRI by assessment of the relation with the surrounding structures.

In most clinical studies the use of fetal MRI looks promising and has evolved as a valuable complementary non-invasive diagnostic method of fetal anatomy and pathology. The current study grouped several indications for MRI of the fetus, and the pathology that benefitted most from supplementary MRI in our study can be compared with the indications resulting from other studies [18, 19, 20, 21].

In our cases, MRI findings were superior compared with US when pathology was situated in the retroperitoneal region: evaluation of renal or extrarenal origin of a mass or confirmation of presence or absence of renal agenesis are some examples. Renal agenesis is associated with a lack of amniotic fluid, which makes ultrasonographic imaging difficult [11].

The MRI contrast in the fetus is strongly dependent on tissue "free" water, and structures such as pericerebral or spinal subarachnoidal spaces, ventricular system, upper and lower airways, lungs, stomach, gallbladder, renal excretion system, and bladder are clearly seen [7, 13]. Visible connection of the extracorporeal cyst with the spinal canal is mandatory in the confirmation of MMC and can be demonstrated with heavily T2-weighted images.

As already reported in the literature, cortical developmental abnormalities, investigation of structural cerebral malformations, and fossa posterior anomalies were other indications for MRI [22, 23, 24].

Assessment of white matter lesions of the fetal brain appeared to be more difficult in 2 cases of our study group, where white matter lesions could be demonstrated with prenatal US. Cystic periventricular leukomalacia and periventricular calcifications with striatal vasculopathy, respectively, in a twin-to-twin transfusion syndrome after laser coagulation (GA 19 weeks) and in a patient with CMV reactivation (GA 33 weeks), were diagnosed on US, respectively, 4 days after and at the time of the MRI. These lesions were not clearly seen on MRI. Since cystic leukomalacia appears usually after 2–4 weeks with a range from 10 to 45 days after the hypoxic–ischemic insult [25], the time delay of 4 days between the MRI and the prenatal US is not a sufficient explanation for not seeing any white matter lesions. The early pregnancy age and small infant is probably the reason for suboptimal MR diagnosis.

The CHD is another indication for evaluation with MR. Advantages of MRI in this severe pathology are confirmation of the localization of the liver and volumetry of the lungs as an additional prognostic factor in assessment of lung hypoplasia [26, 27, 28, 29].

Limitations of our study were the small number of patients and the diverse pathology. Consequently, this study was only observational and retrospective, and no

statistical analysis, neither of the comparison of the MRI findings and ultrasound findings nor of the image quality of the used MR sequences, can be provided.

Conclusion

In conclusion, the use of ultrafast MRI after inconclusive US improved patient counseling and/or pregnancy management in the majority of our patients. Image quality was acceptable, but there is a role for further improvements, focused on image resolution in a small fetus. The use of a HASTE image with long echo time was highly appreciated.

In our study group, fetal MRI was most effective in retroperitoneal pathology, visualization of the airways, assessment of MMC, visualization of the brain parenchyma, and congenital brain malformation with or without associated fossa posterior anomalies.

References

1. Kanal E (1994) Pregnancy and the safety of magnetic resonance imaging. Magn Reson Imaging Clin North Am 2:309–317
2. de Certaines JD, Cathelineau G (2001) Safety aspects and quality assessment in MRI and MRS: a challenge for health care systems in Europe. J Magn Reson Imaging 13:632–638
3. Dempsey MF, Condon B, Hadley DM (2001) Investigation of the factors responsible for burns during MRI. J Magn Reson Imaging 13:627–631
4. Yip YP, Capriotti C, Yip JW (1995) Effects of MR exposure on axonal outgrowth in the sympathetic nervous system of the chick. J Magn Reson Imaging 5:457–462
5. Foster MA, Knight CH, Rimmington JE, Mallard JR (1983) Fetal imaging by nuclear magnetic resonance: a study in goats. Work-in-progress. Radiology 149:193–195
6. McCarthy MS, Filly RA, Stark DD, Callen PW, Golbus MS, Hricak H (1985) Magnetic resonance imaging of fetal anomalies in utero: early experience. AJR 145:677–682
7. Levine D, Hatabu H, Gaa J, Atkinson MW, Edelman RR (1996) Fetal anomaly revealed with fast MR sequences. AJR 167:905–908
8. Ertl-Wagner B, Lienemann A, Strauss A, Reiser MF (2002) Fetal magnetic resonance imaging: indications, technique, anatomical considerations and a review of fetal abnormalities. Eur Radiol 12:1931–1940
9. Girard N (2002) Fetal MR imaging. Eur Radiol 12:1869–1871
10. Bosmans H, Van Hoe L, Gryspeerdt S, Kiefer B, Van Steenbergen W, Baert AL, Marchal G (1997) Single-shot T2-weighted MR imaging of the upper abdomen: preliminary experience with double-echo HASTE technique. AJR 169:1291–1293
11. Goldberg BB (2000) Obstetric US imaging: the past 40 years. Radiology 215:622–629
12. Amin RS, Nikolaidis P, Kawashima A, Kramer LA, Ernst RD (1999) Normal anatomy of the fetus at MR imaging. Radiographics 19: S201–S214
13. Levine D, Barnes PD, Sher S, Semelka RC, Li W, McArdle CR, Worawattanakul S, Edelman RR (1998) Fetal fast MR imaging: reproducibility, technical quality, and conspicuity of anatomy. Radiology 206:549–554
14. Levine D, Barnes PD, Madsen JR, Abbott J, Wong GP, Hulka C, Mehta T, Li W, Edelman RR (1999) Fetal CNS anomalies revealed on ultrafast MR imaging. AJR 172:813–818
15. Chung HW, Chen CY, Zimmerman RA, Lee KW, Lee CC, Chin SC (2000) T2-weighted fast MR imaging with true FISP versus HASTE: comparative efficacy in the evaluation of normal fetal brain maturation. AJR 175:1375–1380
16. Levine D, Barnes PB (1999) Cortical maturation in normal and abnormal fetuses as assessed with prenatal MR imaging. Radiology 210:751–758
17. Huisman TA, Martin E, Kubik-Huch R, Marincek B (2002) Fetal magnetic resonance imaging of the brain: technical considerations and normal brain development. Eur Radiol 12:1941–1951
18. Shinmoto H, Kashima K, Yuasa Y, Tanimoto A, Morikawa Y, Ishimoto H, Yoshimura Y, Hiramatsu K (2000) MR imaging of non-CNS fetal abnormalities: a pictorial essay. Radiographics 20:1227–1243
19. Hubbard AM, Harty MP (2000) MRI for the assessment of the malformed fetus. Baillière's Clin Obstet Gynaecol 14:629–650
20. Whitby E, Paley MN, Davies N, Sprigg A, Griffiths PD (2001) Ultrafast magnetic resonance imaging of central nervous system abnormalities in utero in the second and third trimester of pregnancy: comparison with ultrasound. Br J Obstet Gynaecol 108:519–526
21. Lan LM, Yamashita Y, Tang Y, Sugahara T, Takahashi M, Ohba T, Okamura H (2000) Normal fetal brain development: MR imaging with a half-Fourier rapid acquisition with relaxation enhancement sequence. Radiology 215:205–210
22. Garel C, Brisse H, Sebag G, Elmaleh M, Oury J-F, Hassan M (1998) Magnetic resonance imaging of the fetus. Pediatr Radiol 28:201–211
23. Sonigo PC, Rypens FF, Carteret M, Delezoide A-L, Brunelle FO (1998) MR imaging of fetal cerebral anomalies. Pediatr Radiol 28:212–222
24. Huisman TA, Wisser J, Martin E, Kubik-Huch R, Marincek B (2002) Fetal magnetic resonance imaging of the central nervous system: a pictorial essay. Eur Radiol 12:1952–1961
25. Couture A (1994) Les lésions cérébrales anoxo-ischémiques. In: Couture A, Veyrac C, Baud C (eds) Echographie cérébrale du foetus au nouveau-né. Sauramps Medical, Montpellier, pp 183–248
26. Walsh DS, Hubbard AM, Olutoye OO, Howell LJ, Crombleholme TM, Flake AW, Johnson MP, Adzick NS (2000) Assessment of fetal lung volumes and liver herniation with magnetic resonance imaging in congenital diaphragmatic hernia. Am J Obstet Gynecol 183:1067–1069
27. Rypens F, Metens T, Rocourt N, Sonigo P, Brunelle F, Quere MP, Guibaud L, Maugey-Laulom B, Durand C, Avni FE, Eurin D (2001) Fetal lung volume: estimation at MR imaging: initial results. Radiology 219:236–241
28. Mahieu-Caputo D, Sonigo P, Dommergues M, Fournet JC, Thalabard JC, Abarca C, Benachi A, Brunelle F, Dumez Y (2001) Fetal lung volume measurement by magnetic resonance imaging in congenital diaphragmatic hernia. Br J Obstet Gynaecol 108:863–868
29. Coakley FV, Lopoo JB, Lu Y, Hricak H, Albanese CT, Harrison MR, Filly RA (2000) Normal and hypoplastic fetal lungs: volumetric assessment with prenatal single-shot rapid acquisition with relaxation enhancement MR imaging. Radiology 216:107–111